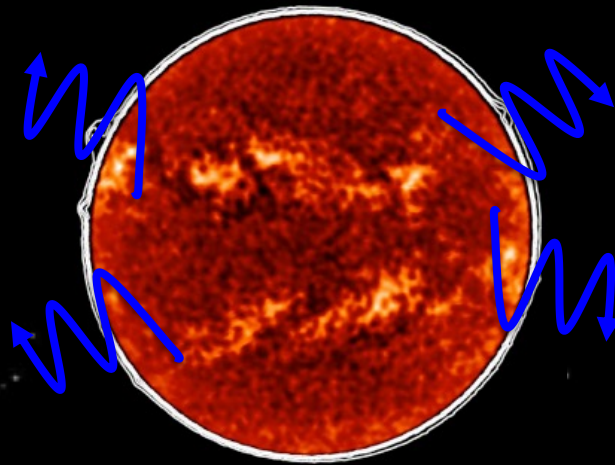


Type III burst fine structure from Langmuir wave motion in turbulent plasma



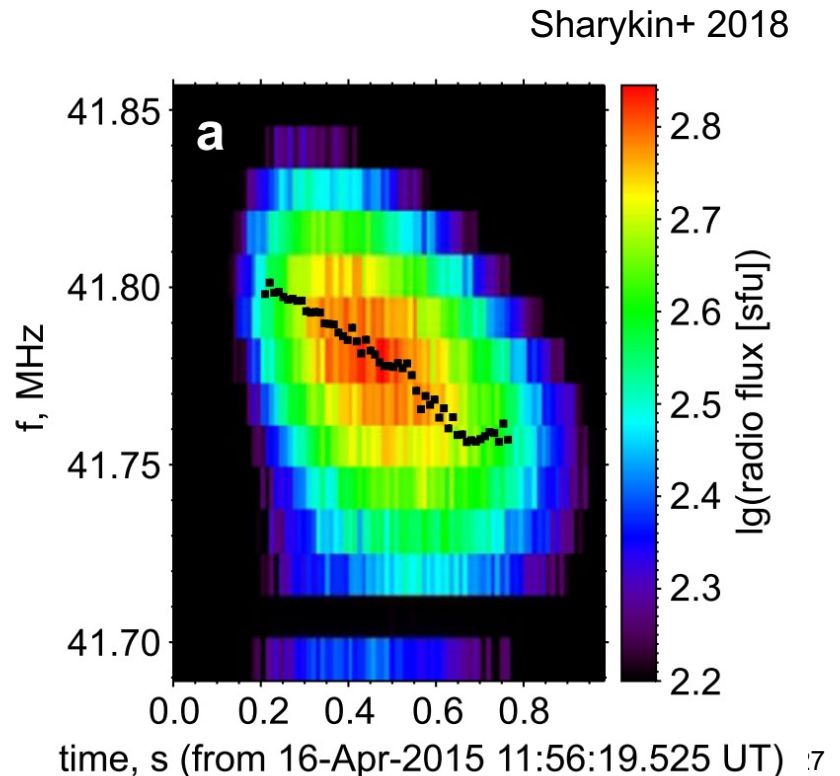
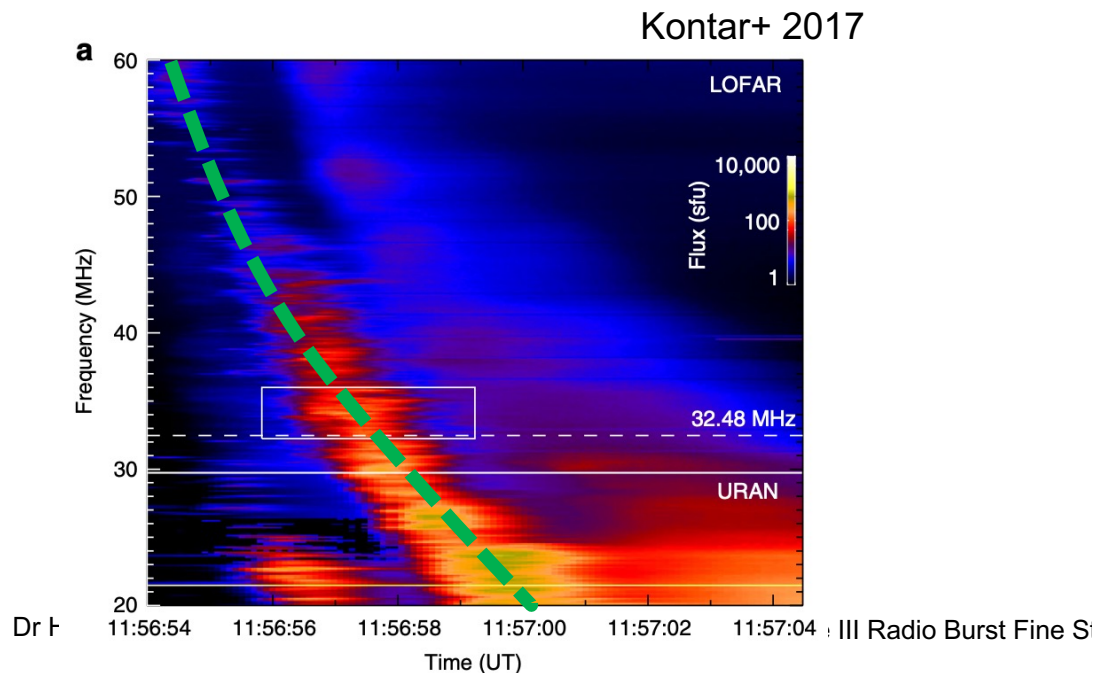
Hamish Reid, Eduard Kontar

hamish.reid@ucl.ac.uk

University College London

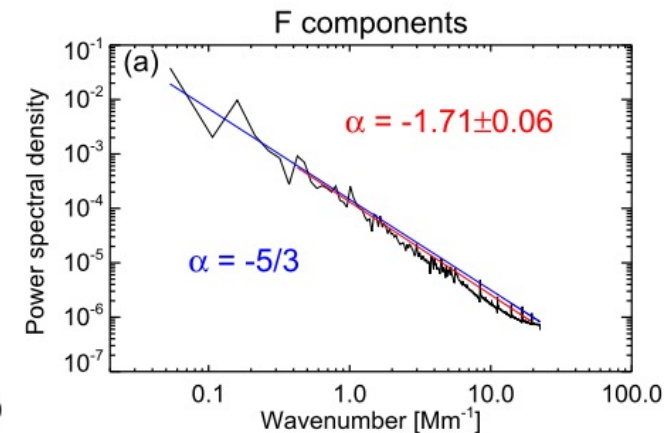
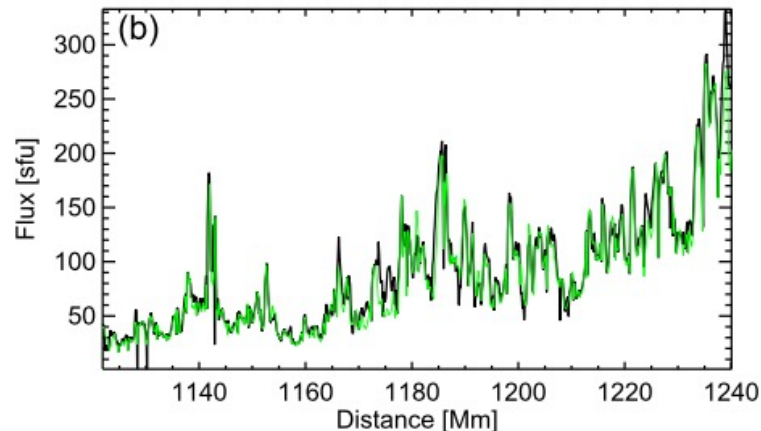
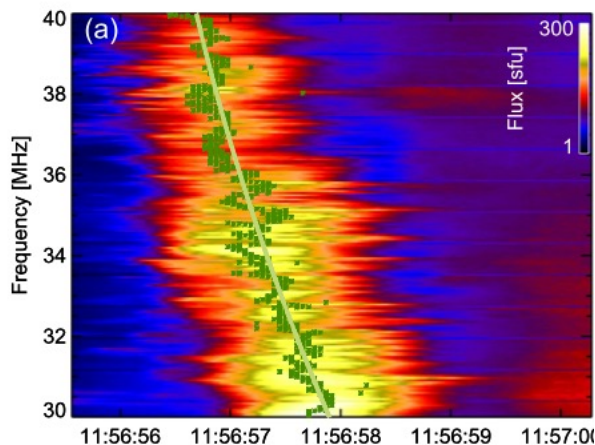
Type III Stria Bursts

- Type III bursts can exhibit fine structure along their backbone (de La Noe et al 1972), named type IIIb burst, or type III striae burst. $t = \text{secs @ 30 MHz}, \frac{\Delta f}{f} = 0.1$
- Stria drift rate infers velocities (0.6 Mm/s) (Sharykin+ 2018). Smaller than beam speeds (100 Mm/s). Larger than sound speed (0.2 Mm/s) (Pecseli 2012).
- What dictates the stria drift rate?
- Why do we care?



Striae Power Spectral Density

- It has long been thought (e.g. Melrose 1986 as a review) that background electron density fluctuations can modulate Langmuir waves and cause radio fine structure.
- Langmuir wave growth can be modulated through wave refraction (e.g. Reid+2010, Li+2012, Loi+2014, Reid+2017).
- Recently, Chen+ 2018 demonstrated the power density spectra of the type III striae peak radio flux obeys a $-5/3$ power-law, very similar to what is observed in situ in the solar wind.

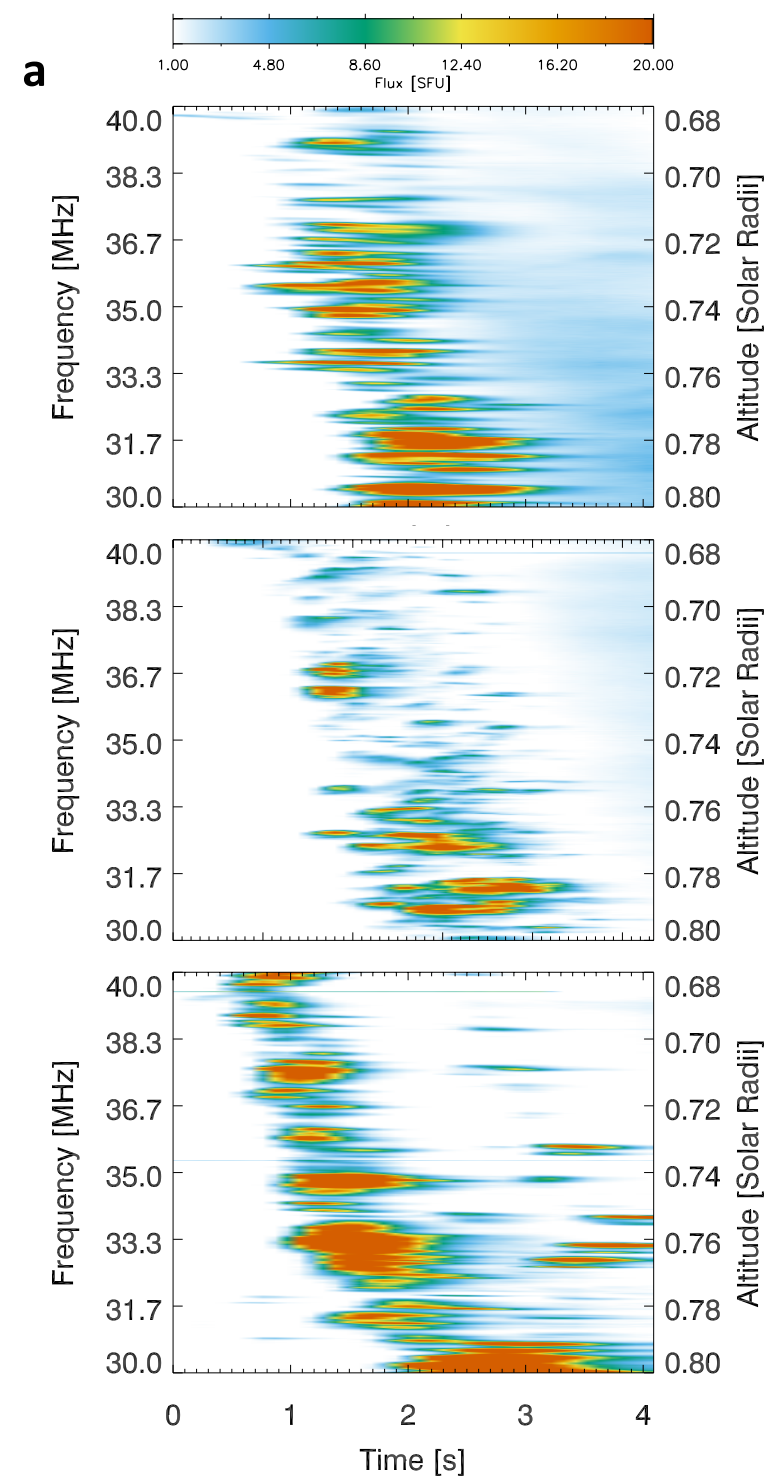


- Nobody has created a robust, theoretical model that links the level and spectrum of density fluctuations from the observed radio spectra.

Type III Striae

- We analyse three type III striae observed by LOFAR. LOFAR allows us to resolve the striae with a very fine frequency resolution, important for resolving striae.
- Three sample events, with the first observed by Kontar+2017, Sharykin+2018 and Chen+ 2018
- Fitting the striae backbone allows us to estimate the electron beam bulk velocity of 88, 49 and 46 Mm/s, respectively.

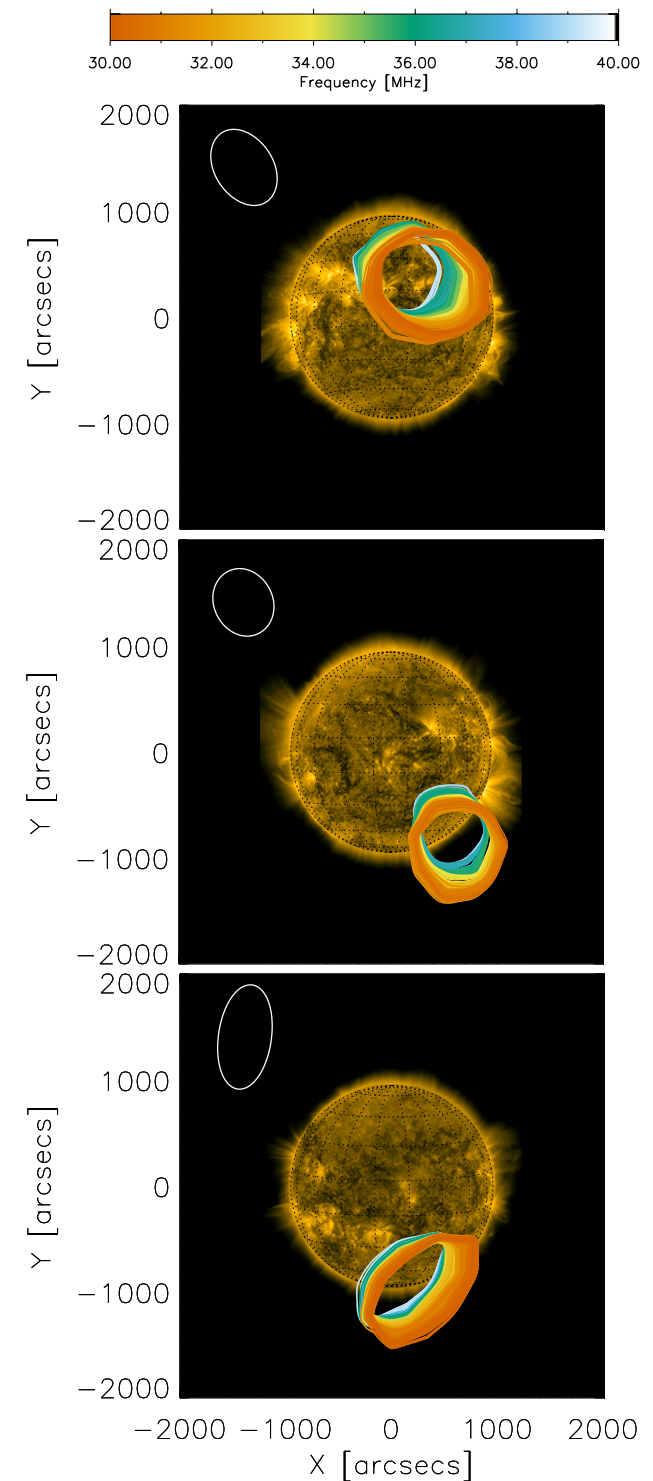
Reid & Kontar 2021, Arxiv: 2103.08424



Type III Striae

- We analyse three type III striae observed by LOFAR. LOFAR allows us to resolve the striae with a very fine frequency resolution, important for resolving striae.
- Three sample events, with the first observed by Kontar+2017, Sharykin+2018 and Chen+ 2018
- Fitting the striae backbone allows us to estimate the electron beam bulk velocity of 88, 49 and 46 Mm/s, respectively.

Reid & Kontar 2021, Arxiv: 2103.08424



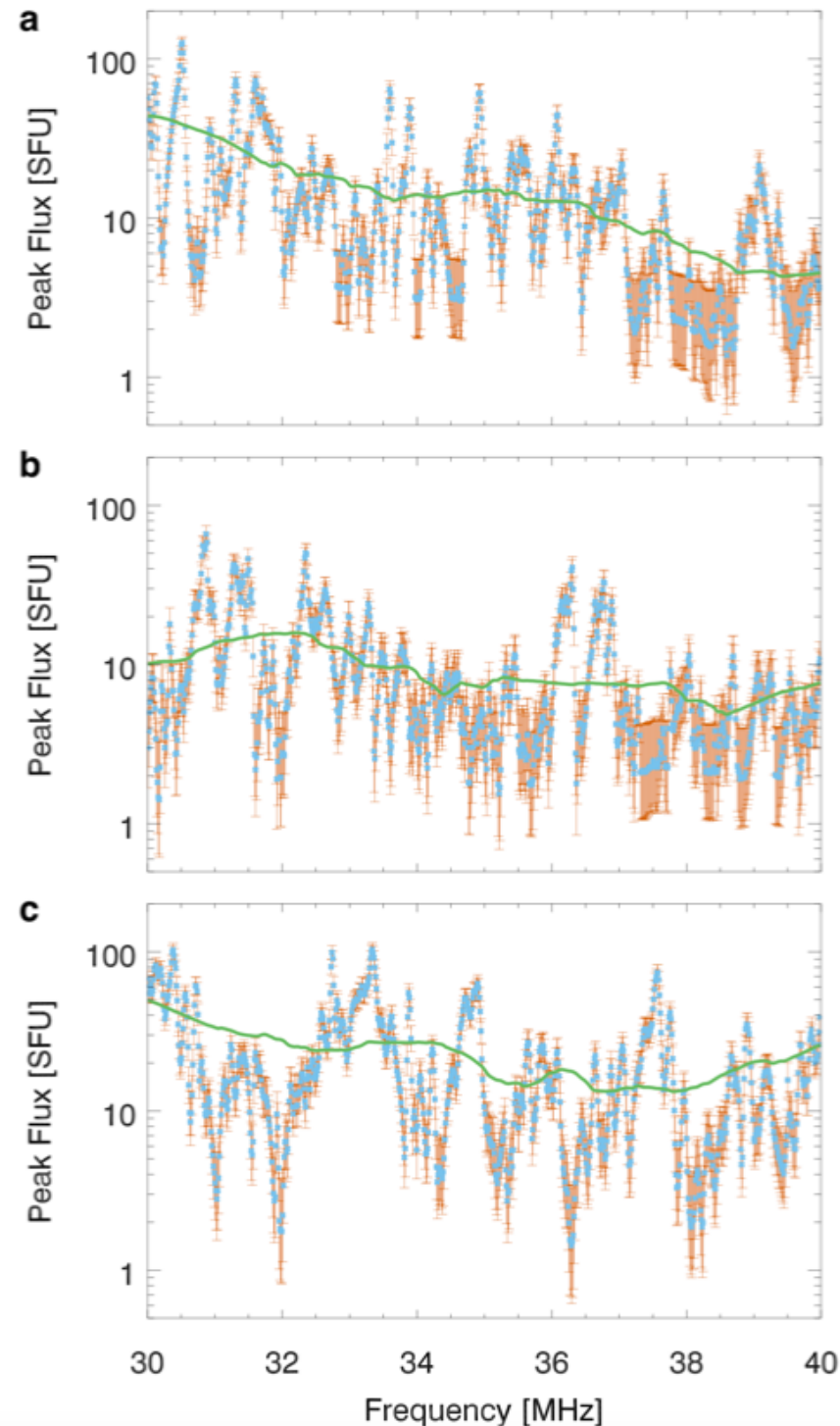
Type II Striae

- We want to characterize the level of fluctuations that occur throughout the striae burst.
- The characteristic intensity of the fine frequency structure is found using

$$\frac{\Delta I}{I} = \left(\frac{\langle (\delta I(\nu))^2 \rangle}{\langle I(\nu) \rangle^2} \right)^{0.5}$$

$I(\nu)$ is the peak flux as a fn of frequency
 $\delta I(\nu)$ is the difference between $I(\nu)$ and the smoothed peak flux.

- $\frac{\Delta I}{I} = 1.41, 1.01, 1.35$, respectively



- The motion of Langmuir waves travelling with a group velocity of $v_{gr} = 3v_{Th}^2/v$ has a shift δv in phase velocity from refraction off density fluctuations with intensity $\Delta n/n$.

$$v_{Th} = \sqrt{k_b T_e / m_e}$$

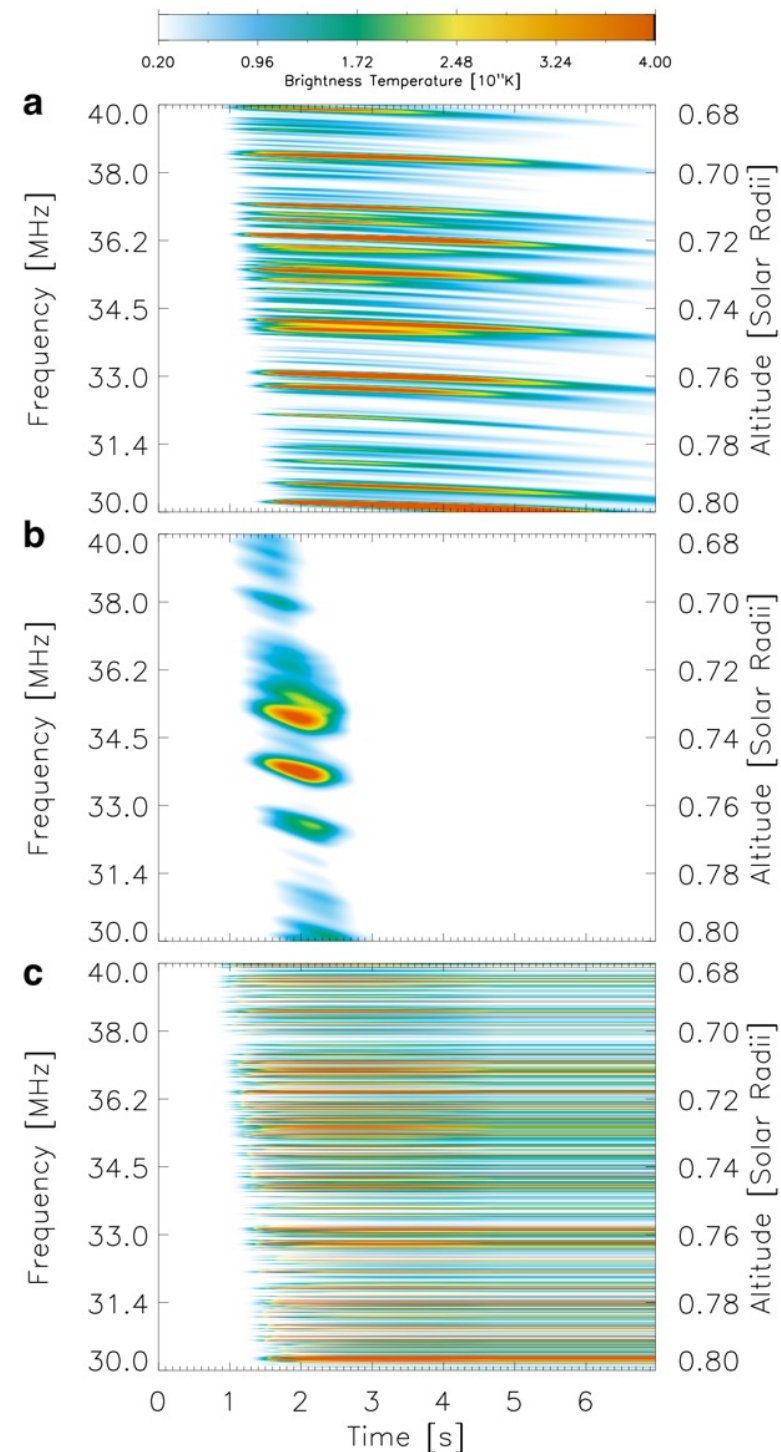
- We have shown that the intensity $\Delta n/n$ can be directly related to the intensity of radio fine structure $\Delta I/I$ via

$$\frac{\langle \Delta n^2 \rangle}{n^2} = \left(\frac{v_{Th}^2}{v_b^2} \right)^2 \frac{\langle \Delta I^2 \rangle}{I^2}$$

- The velocities that dictate the intensity of fluctuations can be viewed as a ratio between the electron beam velocity and Langmuir wave group velocity, as $v_{Th}^2/v_b^2 = v_{gr}/(3v_b)$

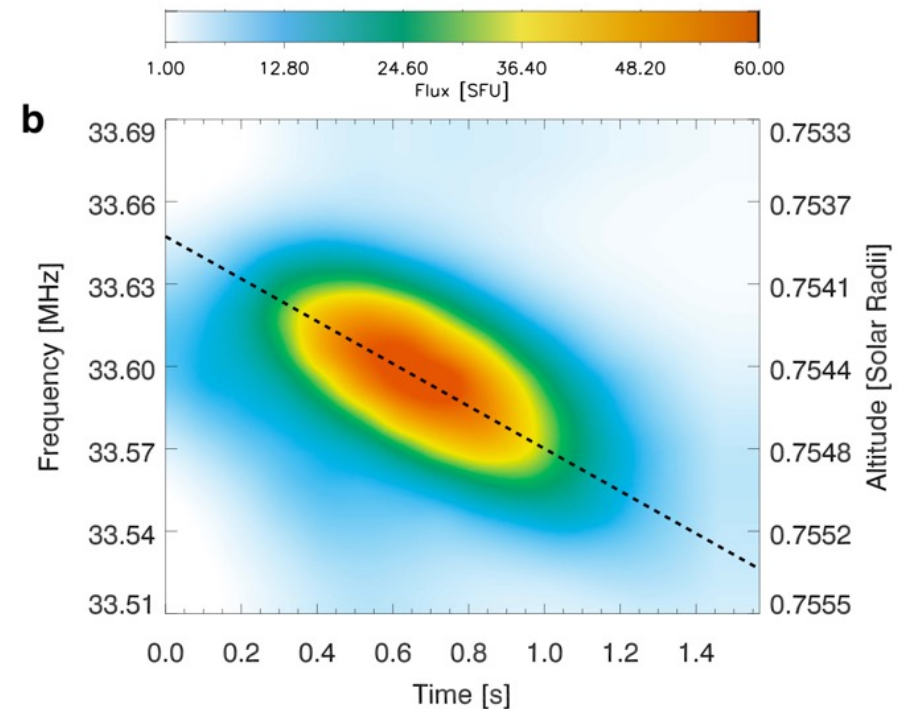
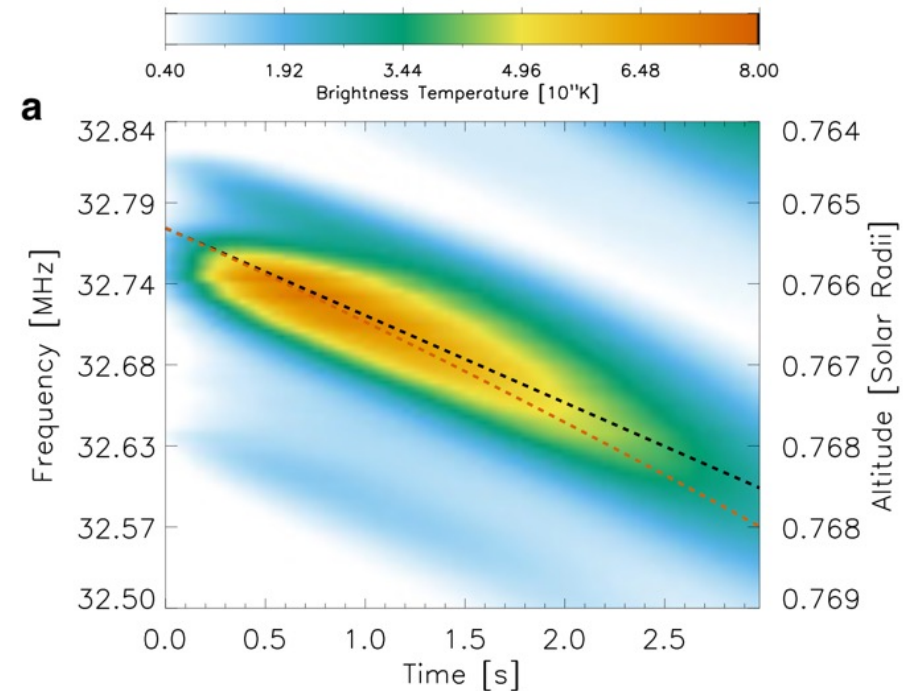
Type III Simulations

- We ran type III simulations out through the corona and created synthetic dynamic spectra.
- Top simulation **(a)** is 1 MK plasma. Striae look similar to obs but are slightly too long duration. Mostly realistic.
- Middle simulation **(b)** is 10 MK plasma. Striae are too fat in frequency but are shorter. Not realistic.
- Bottom simulation **(c)** has no group velocity. Frequency fine structure is not realistic.



Stria Velocity

- Striae between observation and simulations are similar.
- Simulated stria **(a)** derived velocity is 0.6 Mm/s, or 0.63 to 0.76 Mm/s using a quadratic. Drifting at the Langmuir wave group velocity.
- Observed stria **(b)** derived velocity is 0.69 Mm/s. Data is interpolated to increase resolution for clarity.



- Striae drifting at the Langmuir wave group velocity is significant.

$$\frac{\partial f}{\partial t} = \frac{f}{2n_e} \frac{\partial n_e}{\partial x} v_b$$

Type III backbone drift rate

$$\frac{\partial f_s}{\partial t} = \frac{f}{2n_e} \frac{\partial n_e}{\partial x} \frac{3v_{Th}^2}{v_b}$$

Type III stria drift rate

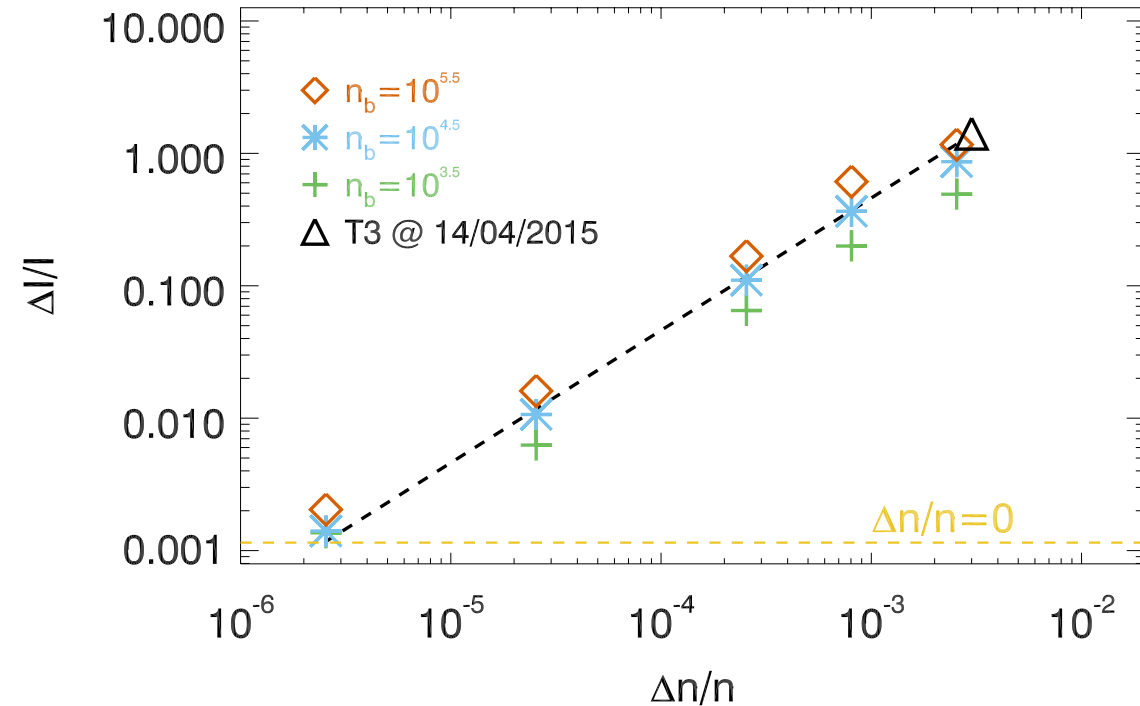
- Assuming the background density model (dn_e/dx), we can obtain v_b and so derive v_{Th} , and hence the solar coronal temperature.

- Sharykin+ 2018 found velocity from average stria of 0.58 Mm/s. With the beam velocity of 88 Mm/s gives a thermal velocity of

$$v_{Th} = \sqrt{v_{gr} v_b / 3} = 4.1 \text{ Mm s}^{-1} \text{ which gives } T = 1.1 \text{ MK.}$$

Frequency Fine Structure

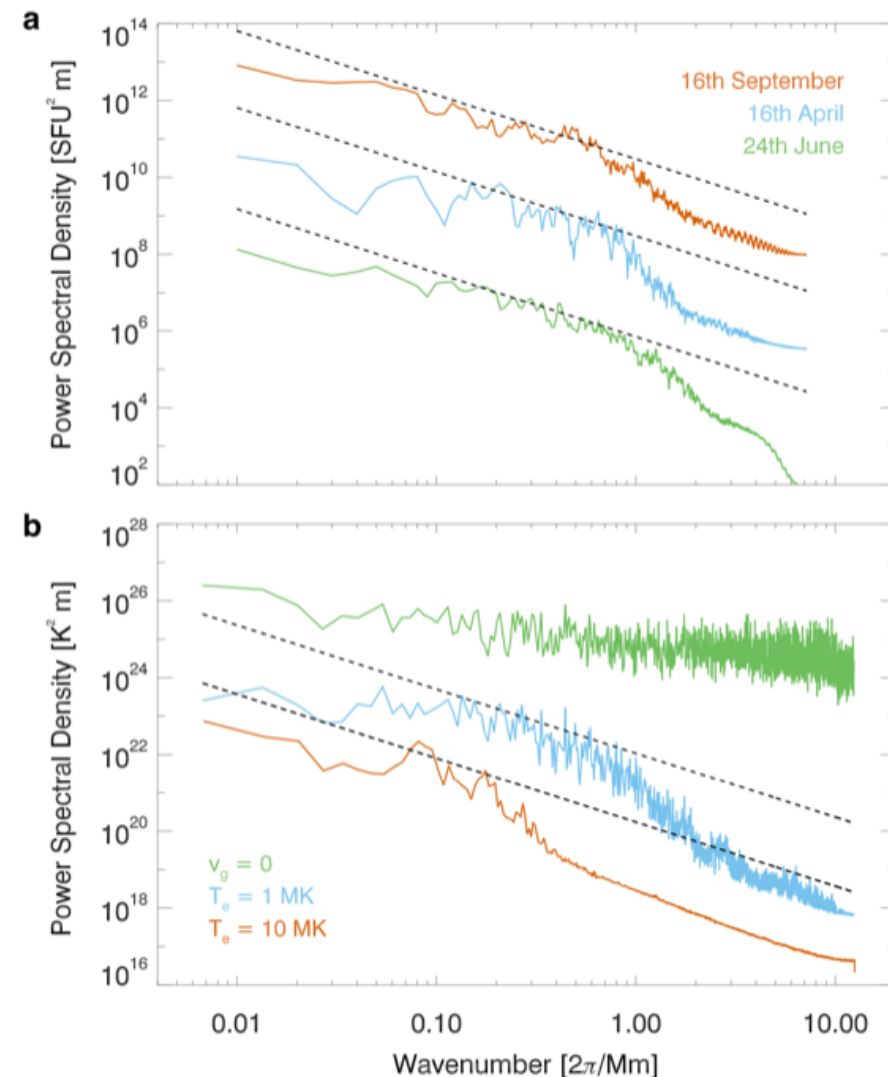
- Multiple simulations with different initial beam densities and levels of background density turbulence.
- The simulations confirm the initial relation between $\Delta n/n$ and $\Delta I/I$.
- Observations given $\Delta I/I = 1.41$ $v = 88$ Mm/s , $v_{Th} = 4.1$ Mm/s gives $\Delta n/n = 0.3\%$.



$$\frac{\langle \Delta n^2 \rangle}{n^2} = \left(\frac{v_{Th}^2}{v^2} \right)^2 \frac{\langle \Delta I^2 \rangle}{I^2}$$

Type III Power Spectra Density

- Power Spectral Density for the observed (a) and simulated (b) type III dynamic spectra.
- Fluctuations obey a roughly $-5/3$ spectral index. Decrease in power at the small spatial scales. Caused by smoothing at the Langmuir wave group velocity.
- When group velocity is zero, the fluctuations are unrealistic.



Reid & Kontar 2021, Arxiv: 2103.08424

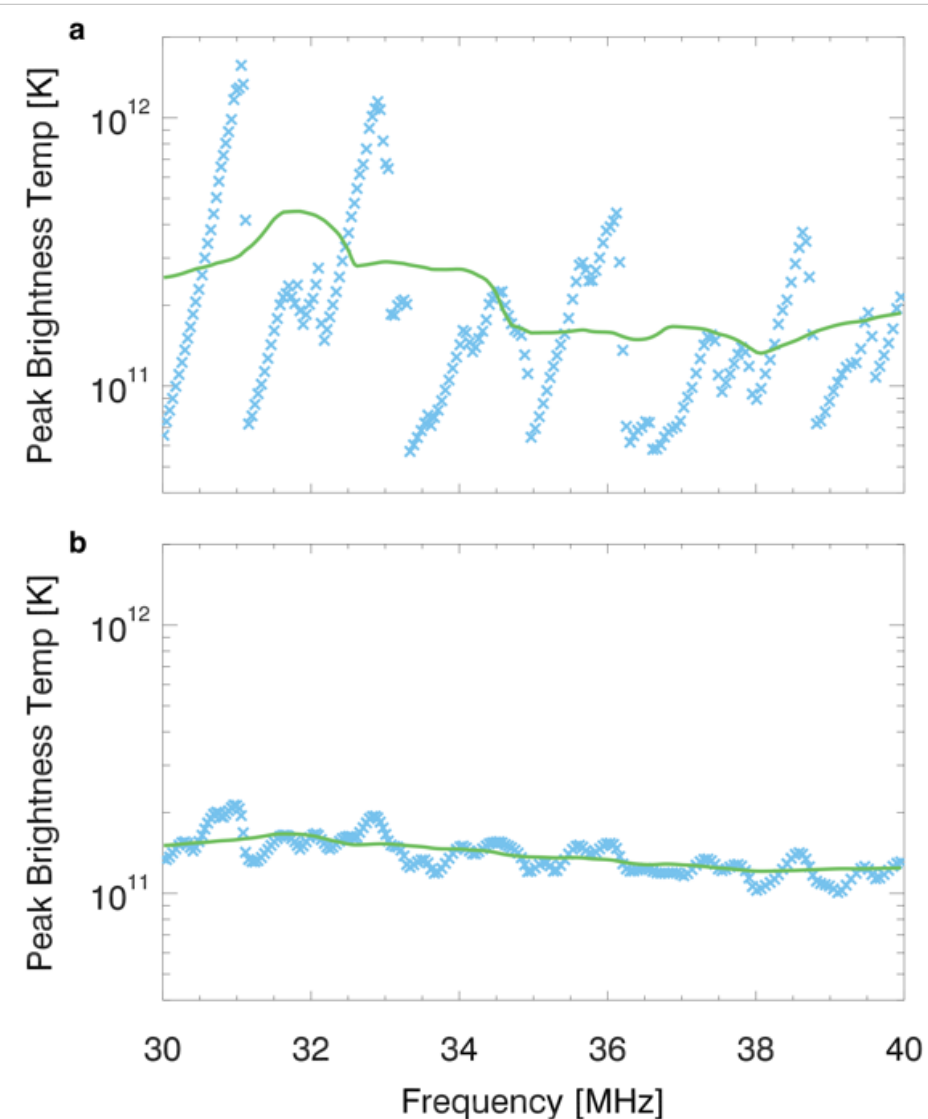
- Radio fine structure intensity can provide a diagnostic of the spectra and intensity of background density turbulence via $\Delta I/I = (v_{\text{Th}}^2/v_b^2)\Delta n/n$, and we inferred levels around 0.1 - 0.3%.
- Fine structure can also constrain the plasma temperature, where we find 1.1 MK plasma at heights around 0.8 solar radii.
- Enhanced resolution of Parker Solar Probe and Solar Orbiter can measure radio fine structure at lower frequencies. Can help infer the radial evolution of density turbulence close to the Sun.

Frequency Fine Structure

- Simulated striae intensity was found in the same way as the observations.

$$\frac{\Delta I}{I} = \left(\frac{\langle (\delta I(\nu))^2 \rangle}{\langle I(\nu) \rangle^2} \right)^{0.5}$$

- Simulations show the increase in fine structure when the background density turbulence is increased.

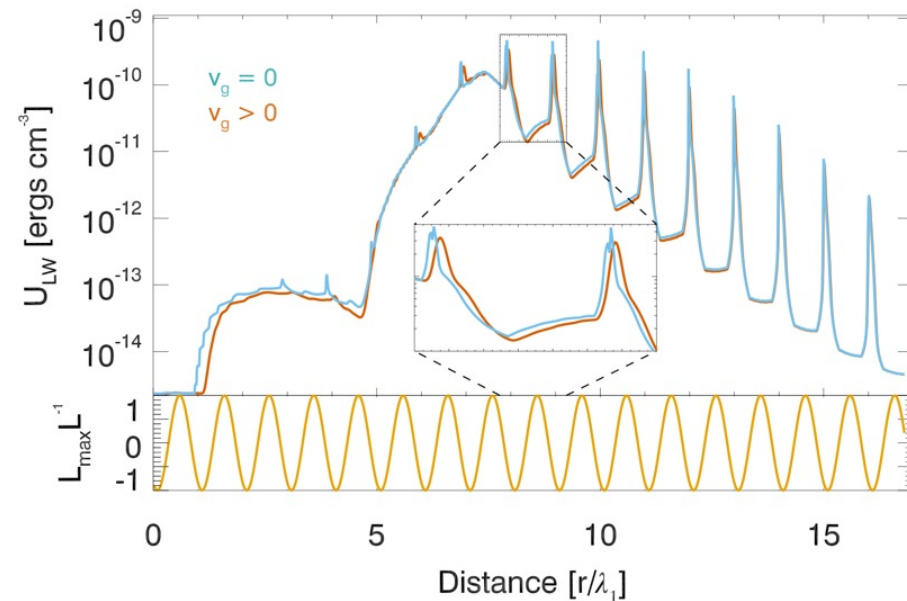
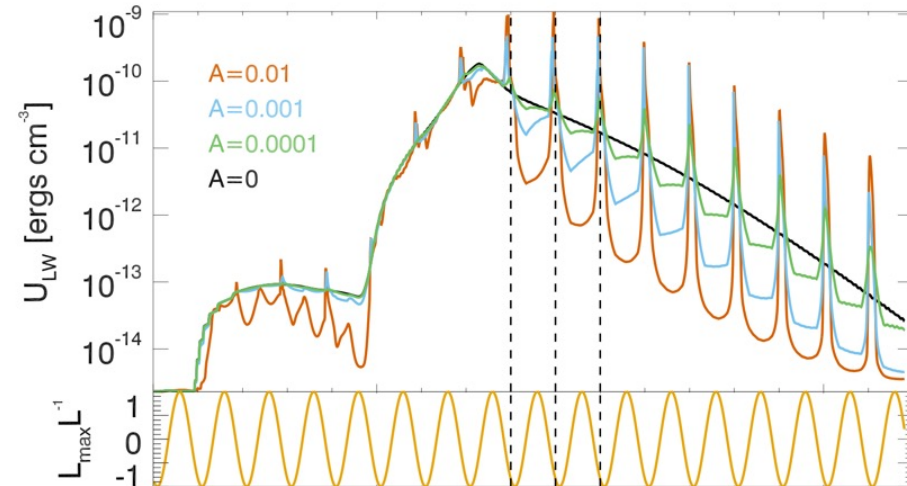


Langmuir Wave Modulation

- We ran electron beam simulations propagating through the ‘corona’. Mean background plasma was constant. We added a sinusoidal perturbation.

$$n_e(x) = n_0(1 + A \sin(k_1 x + \phi)),$$

- Resultant Langmuir wave energy density was modulated. Larger values of A give larger modulation.
- Inclusion of Langmuir wave group velocity leads to phase difference between waves and background.

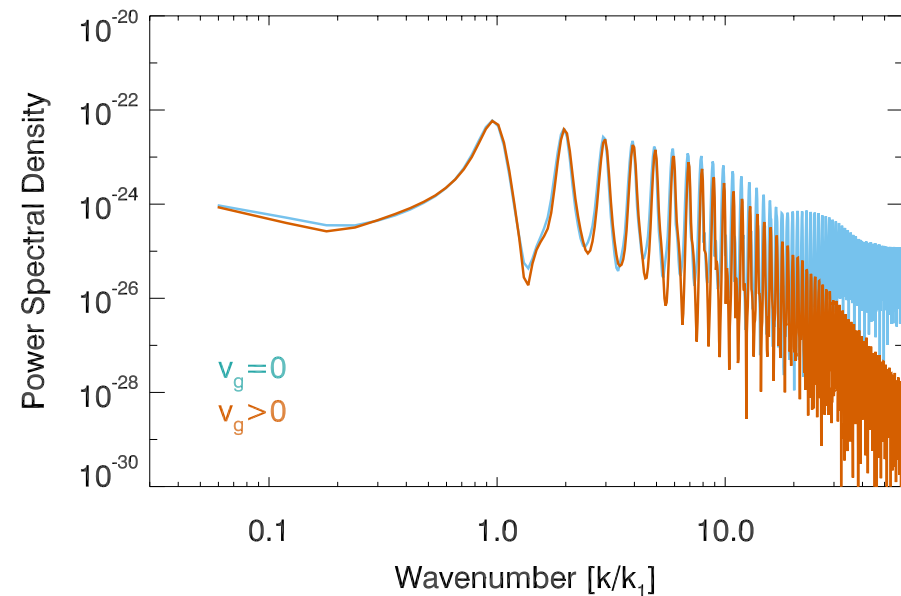
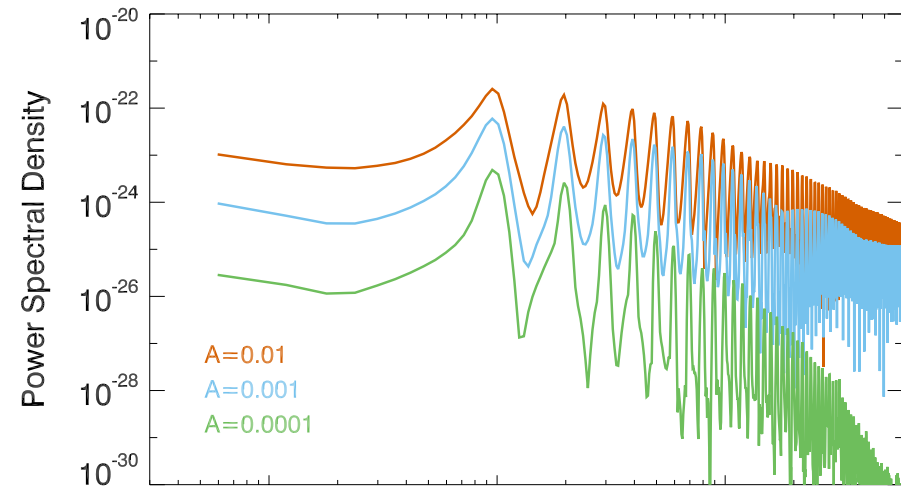


Langmuir Wave Modulation

- We ran electron beam simulations propagating through the ‘corona’. Mean background plasma was constant. We added a sinusoidal perturbation.

$$n_e(x) = n_0(1 + A \sin(k_1 x + \phi)),$$

- Resultant Langmuir wave energy density was modulated. Larger values of A give larger modulation.
- Inclusion of Langmuir wave group velocity damps fluctuations at higher wavenumbers (smaller scale)



- **1D Kinetic code that simulates the propagation of electrons along the magnetic field and their resonant wave-particle interaction with Langmuir waves.**

$$\frac{\partial f}{\partial t} + \frac{v}{M(r)} \frac{\partial}{\partial r} M(r) f = \frac{4\pi^2 e^2}{m_e^2} \frac{\partial}{\partial v} \left(\frac{W}{v} \frac{\partial f}{\partial v} \right) + \frac{4\pi n_e e^4}{m_e^2} \ln \Lambda \frac{\partial}{\partial v} \frac{f}{v^2} + S(v, r, t)$$

$$\frac{\partial W}{\partial t} + \frac{\partial \omega_L}{\partial k} \frac{\partial W}{\partial r} - \frac{\partial \omega_{pe}}{\partial r} \frac{\partial W}{\partial k} = \frac{\pi \omega_{pe}}{n_e} v^2 W \frac{\partial f}{\partial v} - (\gamma_L + \gamma_c) W + e^2 \omega_{pe} v f \ln \frac{v}{v_{Te}}$$

Propagation, Coulomb collisions, quasilinear wave growth and diffusion, wave refraction, spontaneous emission, source function.

e.g. Reid & Kontar 2018

Distribution function
varies with velocity as
a power-law $\alpha = 7$

$$f(v, r, t) = Av^{-\alpha} \exp\left(\frac{-(r - r_{inj})^2}{d^2}\right) \exp\left(\frac{-(t - t_{inj})^2}{\tau^2}\right)$$

Distribution function
varies as a Gaussian in
position space

$$d = 10Mm$$

Distribution function
varies as a Gaussian in
time with different rise
and decay times

$$\tau_{rise} = \tau_{decay} = 0.001s$$

- The initial level of Langmuir wave spectral energy density is defined as:

$$W_{Th}(v, r, t = 0) = \frac{k_B T_e}{4\pi^2} \frac{\omega_{pe}(r)^2}{v^2} \log\left(\frac{v}{v_{Te}}\right),$$

- To obtain the energy density we integrate the spectral energy density over k :

$$E_w(r, t) = \int W(k, r, t) dk = \int \frac{\omega_{pe}}{v^2} W(v, r, t) dv.$$

- As the magnetic field expands the electron cloud rarefies. We model the radial expansion by using

$$M(r) = (r + r_0)^\beta$$

- where β determines the rate of radial expansion and r_0 determines the base of the conical expansion.
- The base, $r_0=3.5 \times 10^9$ cm and makes a cone of 33° when $\beta=2$.

- The background density model remains static in time due to the high energy electrons moving much faster.
- We use the Parker 1958 density model with normalisation constant from Mann et al 1999.

$$r^2 n_0(r) v(r) = C = \text{const},$$

$$\frac{v(r)^2}{v_c^2} - \ln\left(\frac{v(r)^2}{v_c^2}\right) = 4 \ln\left(\frac{r}{r_c}\right) + 4 \frac{r_c}{r} - 3,$$

Generally, we add density fluctuations to a power density spectra more realistic to the solar wind.

$$\delta n(x) = \langle n(x) \rangle C \sum_{n=1}^N \lambda_n^{\beta/2} \sin(2\pi x / \lambda_n + \phi_n)$$

The constant C is normalised to the value of $\langle \delta n(x) \rangle$ near the Earth (Celnikier et al 1987)

$$C = \sqrt{\frac{2 \langle \delta n(x)^2 \rangle}{\langle n(x) \rangle^2 \sum_{i=1}^N \lambda_i^\beta}}$$

Fluctuations close to the Sun are made less prolific than density fluctuations close to the Earth.

$$\frac{\langle \delta n(x_1)^2 \rangle}{\langle n(x_1) \rangle^2} = \left(\frac{n(1AU)}{n(x_2)} \right)^\psi \frac{\langle \delta n(x_2)^2 \rangle}{\langle n(x_2) \rangle^2}$$

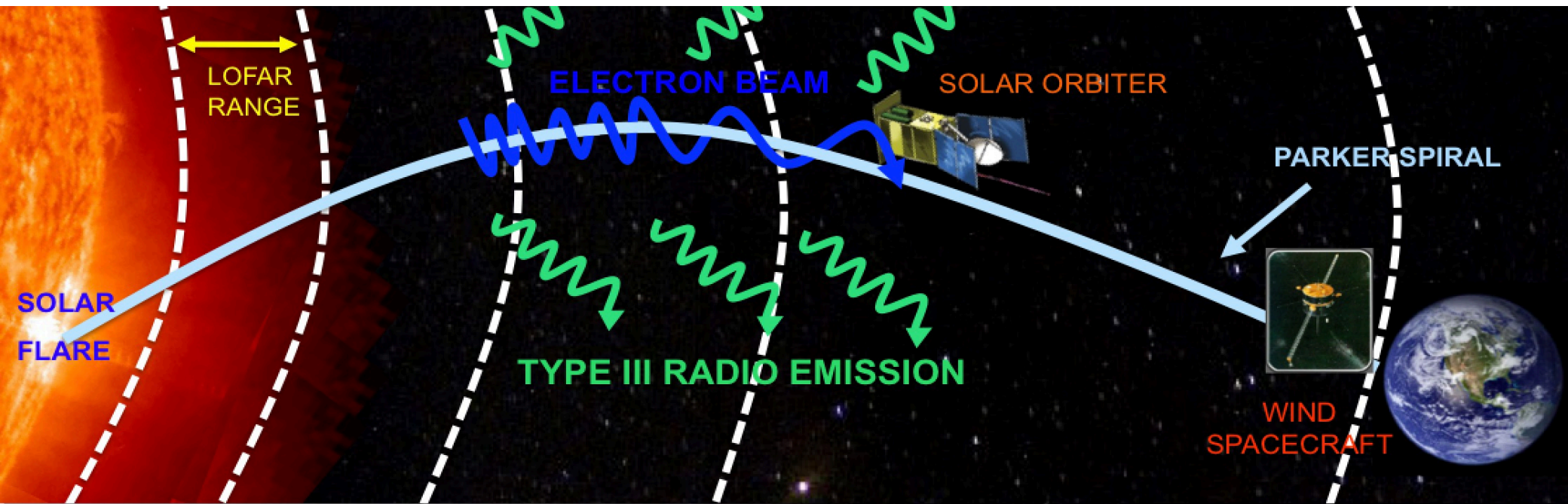
$$\psi \geq 0$$

- Assume the process $L+S \rightarrow T$, or the coalescence of a Langmuir wave and an Ion Sound wave into a Transverse wave close to the background plasma frequency.
- If there is a bath of Ion Sound waves, the brightness temperature of fundamental emission depends upon Langmuir wave spectral energy density

$$k_b T_T(k, r, t) \approx \frac{(2\pi)^2}{k_L(r)^2} W_L(k, r, t)$$

Solar Electron Beams

Solar electron beams propagate through the heliosphere, can be detected in-situ and via type III radio bursts. Theory by Ginzburg & Zhelezniakov 1958. Review by Reid & Ratcliffe 2014. Recent type III imaging spectroscopy review by Reid 2020.



250 MHz	10 MHz	1 MHz	0.15 MHz	0.02 MHz
0.16 R_{SUN}	1.5 R_{SUN}	7.5 R_{SUN}	0.18 AU	1.2 AU
1.2×10^8 m	10^9 m	5.7×10^9 m	2.7×10^{10} m	1.8×10^{11} m
MID CORONA	HIGH CORONA	INTER-PLANETARY SPACE	ORBIT OF MERCURY	PARKER SPIRAL LENGTH AT EARTH

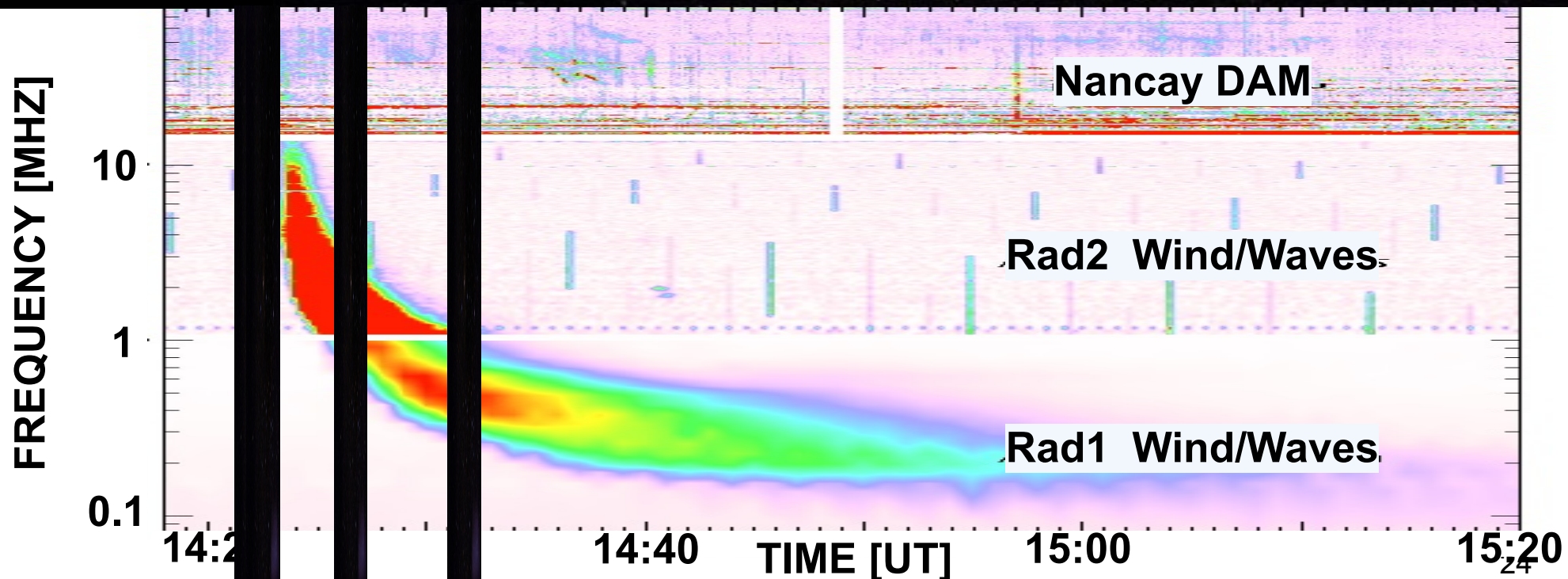
Slow
(e.g. 0.1c)

Electron Beam Velocity

Fast
(e.g. 0.4c)

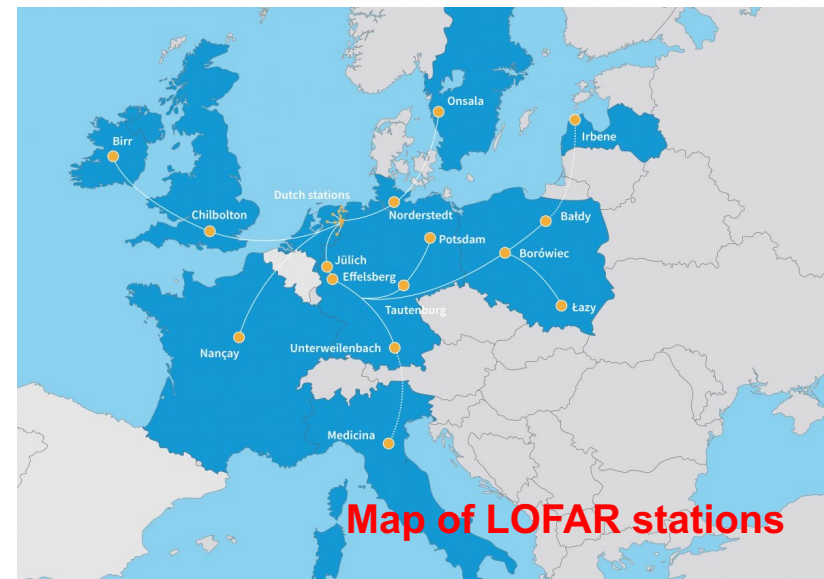


Over time, beams expand, background density and type III frequency decreases

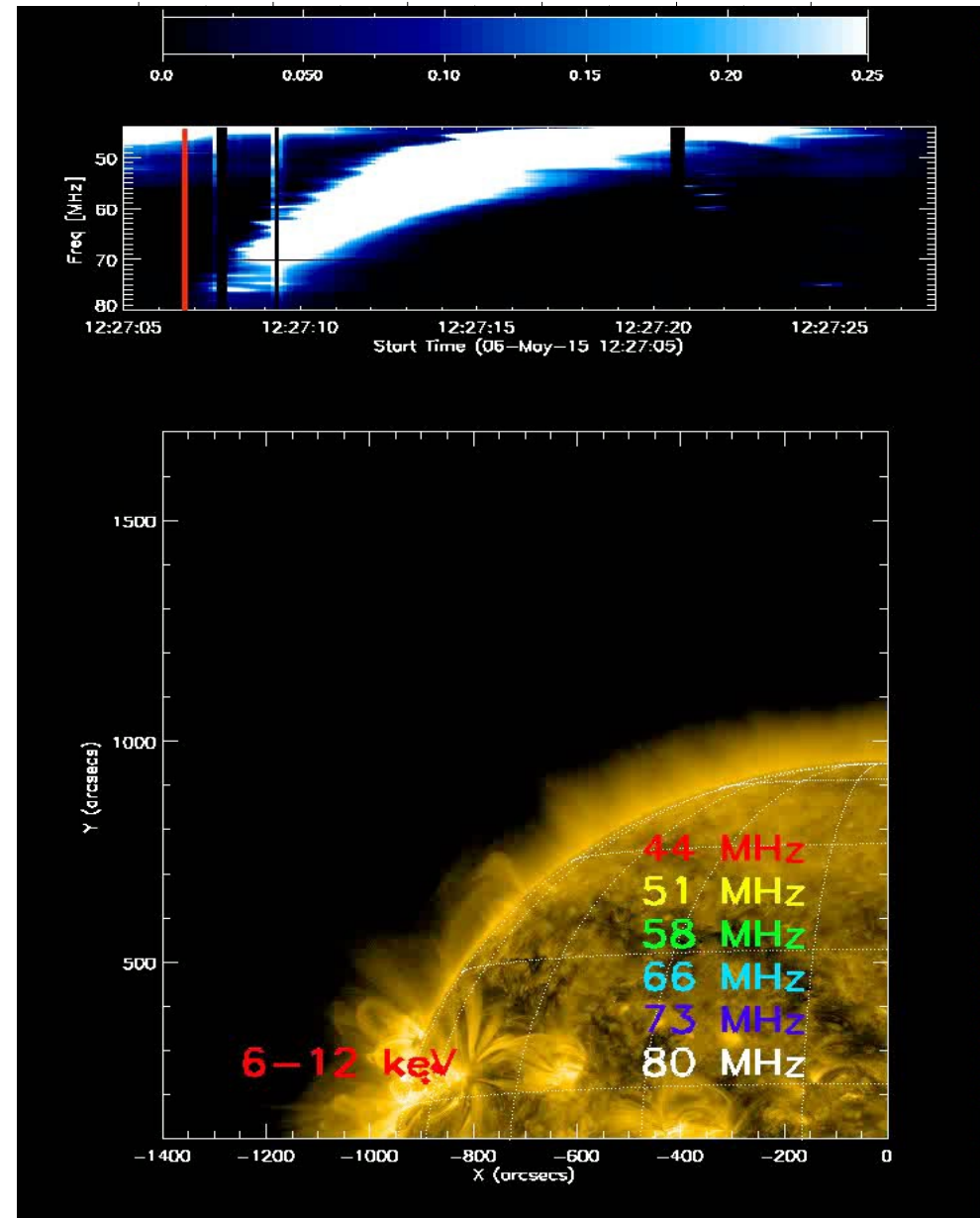


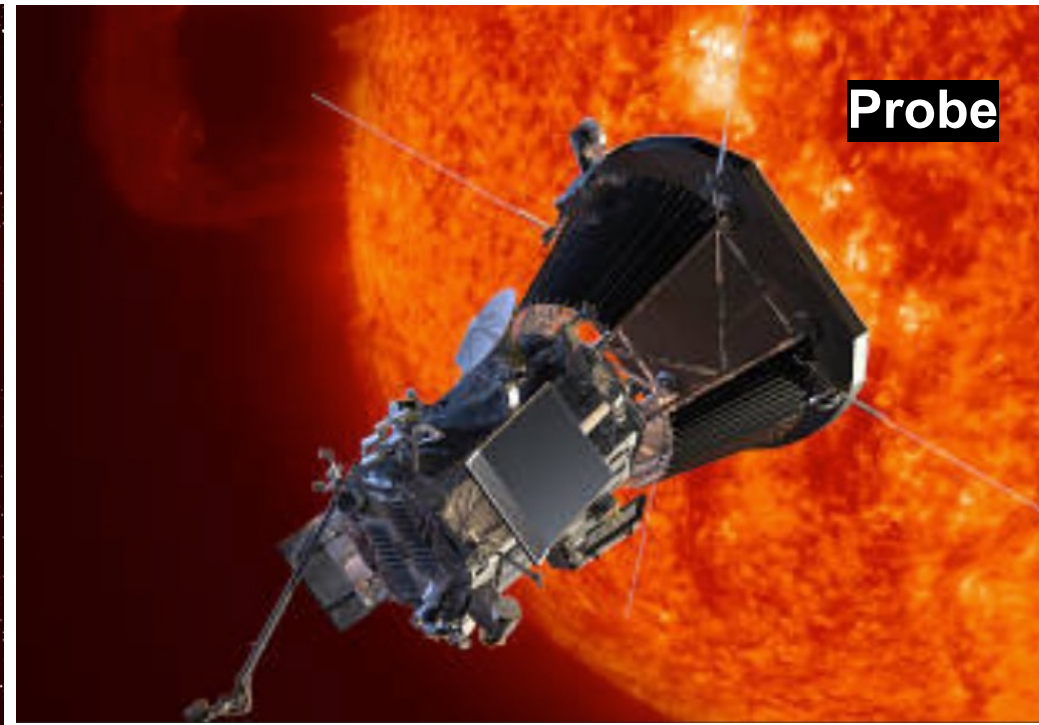
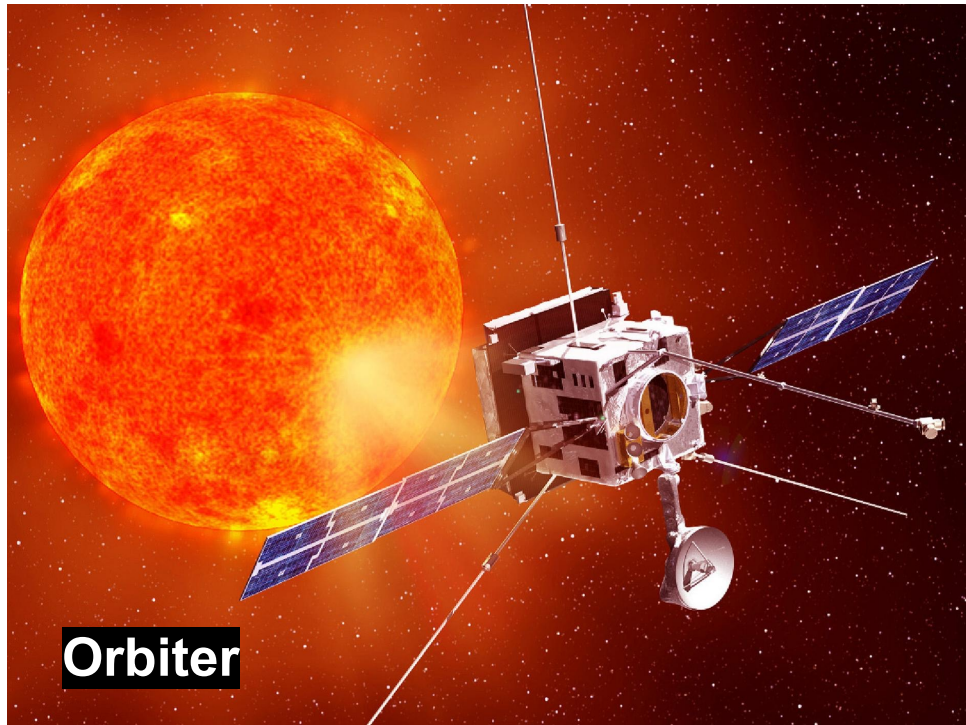
Low Frequency ARray (LOFAR)

- LOFAR is an interferometer made up of many stations, centred in Netherlands and distributed through Europe.
- Operated between 10-250 MHz
- Sub-second time resolution
- 10s kHz frequency resolution
- Arcsec spatial resolution (not req. for Sun)
- Observes at EU daytime (e.g. 07-16 UT)
- LOFAR requires proposal time to observe the Sun – typically we observed during PSP perihelions and will have made cases for coordinated SoLO campaigns.



- Electron beams that make type IIIs can derive density profiles within the corona.
- U-bursts/Type IIIs can image large coronal structures at 1+ solar radii (e.g. Reid & Kontar 2017).





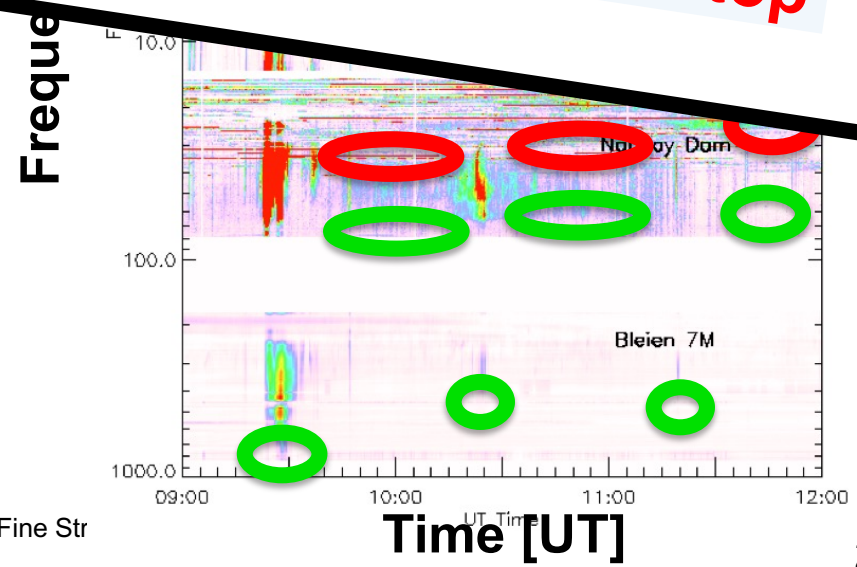
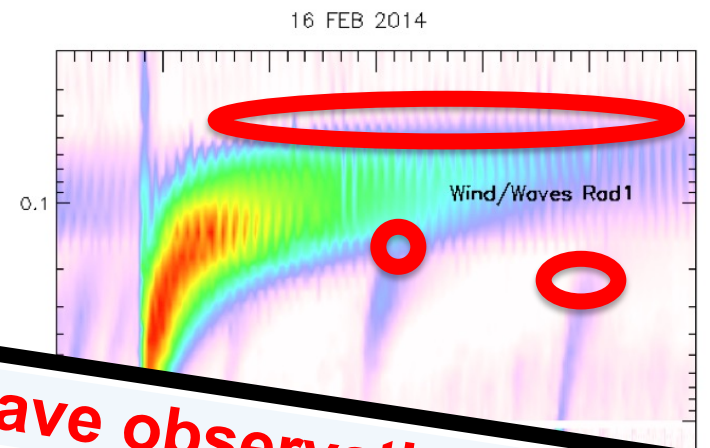
- Solar Orbiter and Parker Solar Probe measuring in situ particles and electromagnetic fields close to the Sun!
- (Non-)thermal electron distributions, Langmuir waves, density turbulence, radio + UV + X-rays.
- **What solar electron beam science questions can be answered?**

Starting and Stopping Frequency

- Electron beams stimulate type III bursts that have spectral

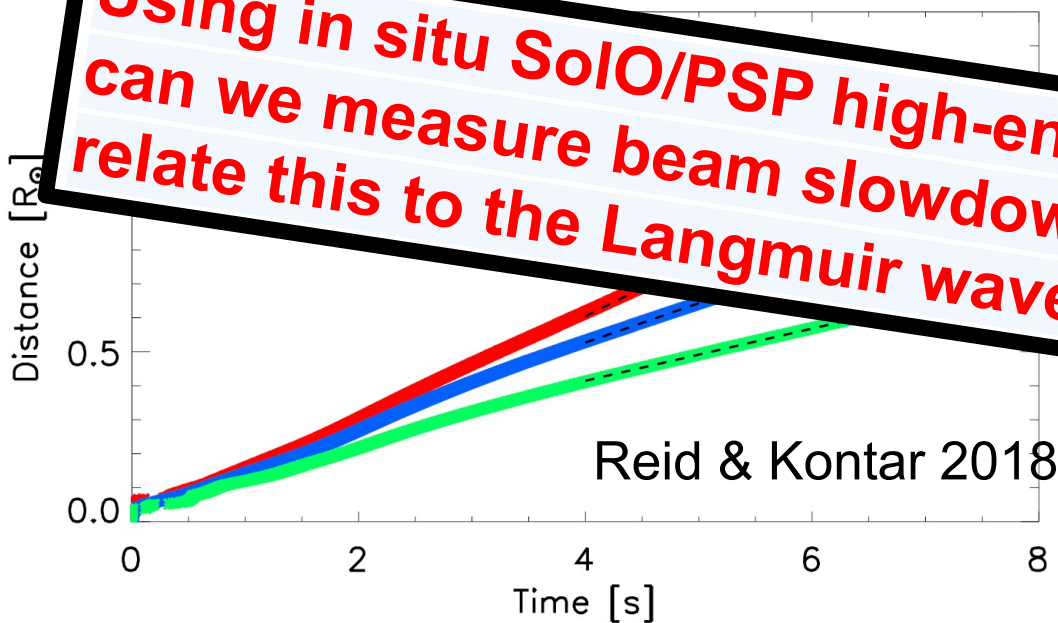
Using in situ SoLO/PSP electron/wave observations, can we confirm the beam property dependencies with start/stop type III frequencies?

- **Stopping frequency**
Reid & Kontar 2015
- **Starting frequency**
Reid et al 2011, 2014, 2017c

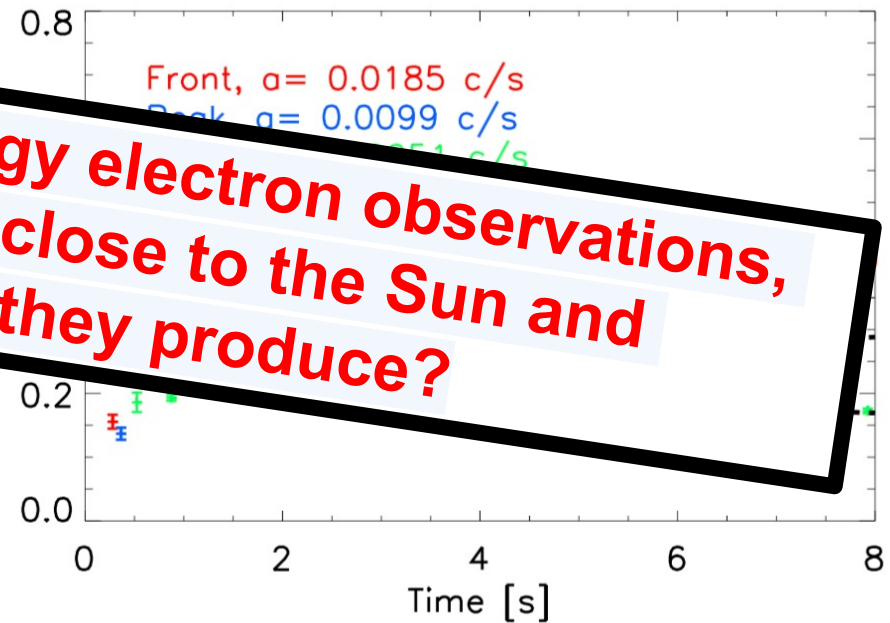


- Exciter speeds from type III bursts have been observed to slow down in the heliosphere (e.g. Dulk+ 1998, Krupar+ 2015).
- Simulations show exciter speed-up close to the Sun.

Using in situ SOLO/PSP high-energy electron observations, can we measure beam slowdown close to the Sun and relate this to the Langmuir waves they produce?



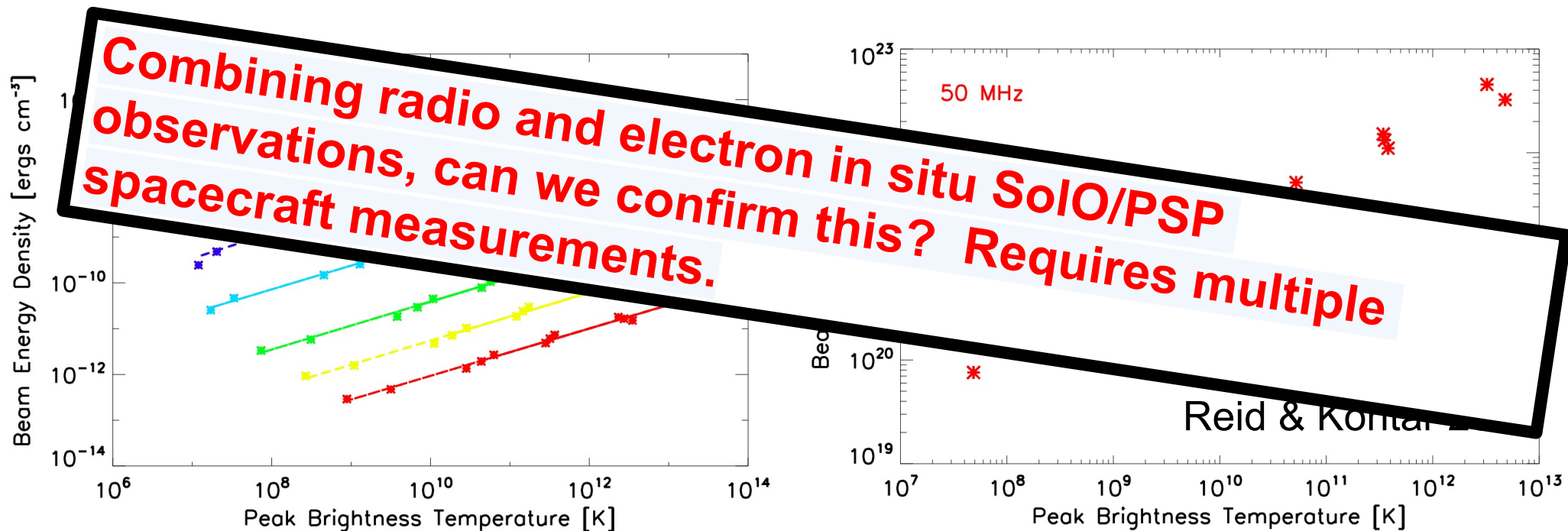
Linear fit to the positions in time derives constant velocities.



Linear fit to the velocities derives constant (de)acceleration.

- Langmuir waves arrive with electrons $< 10 \text{ keV}$ at 1 AU but what about closer?

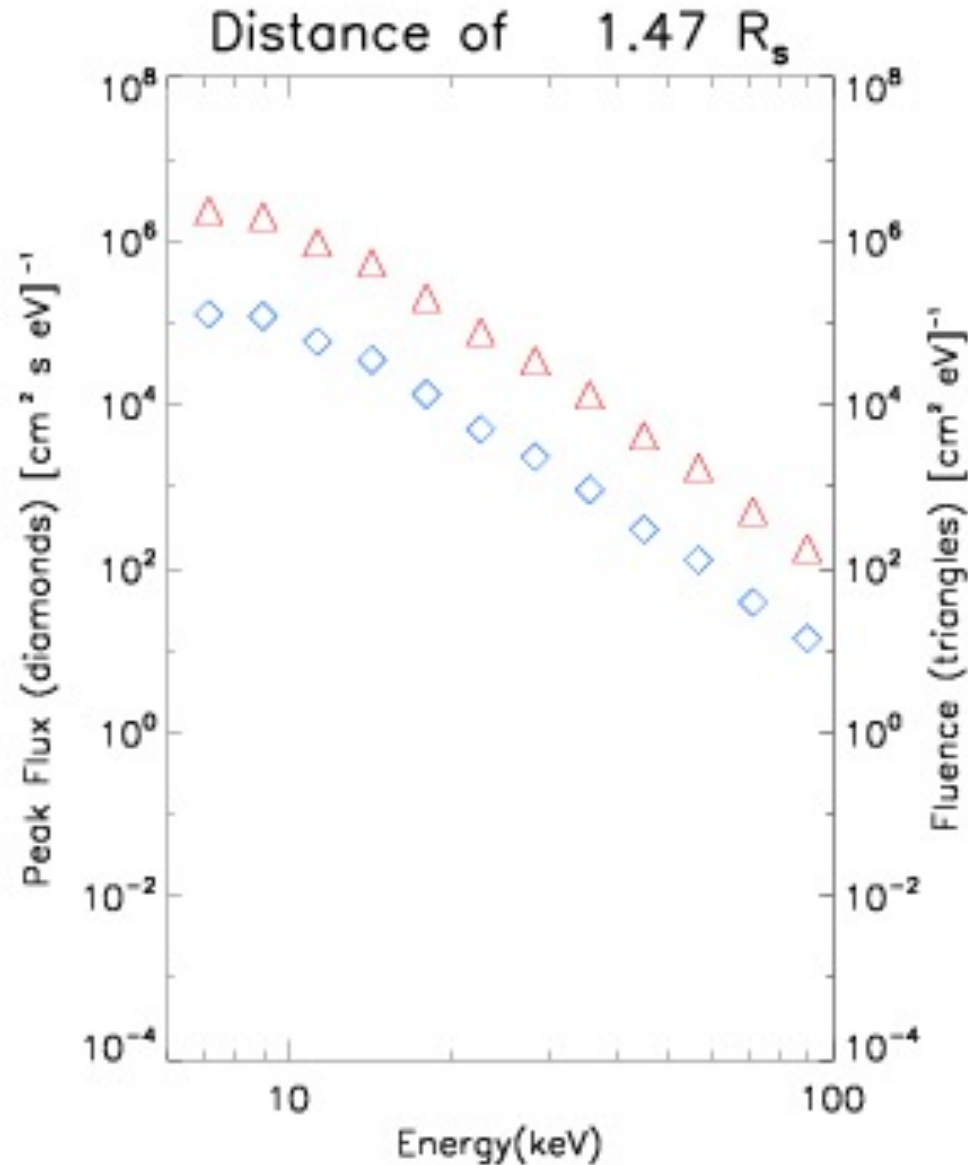
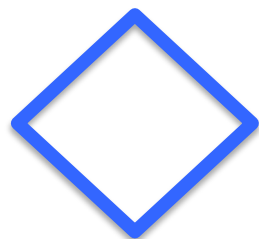
- Simulations predicted that the energy density of electrons is proportional to the type III peak brightness temperature.



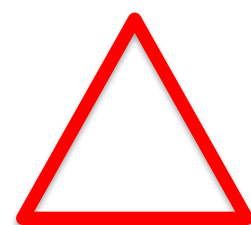
- Can make some assumptions to estimate beam energy.

Electron Spectra Evolution

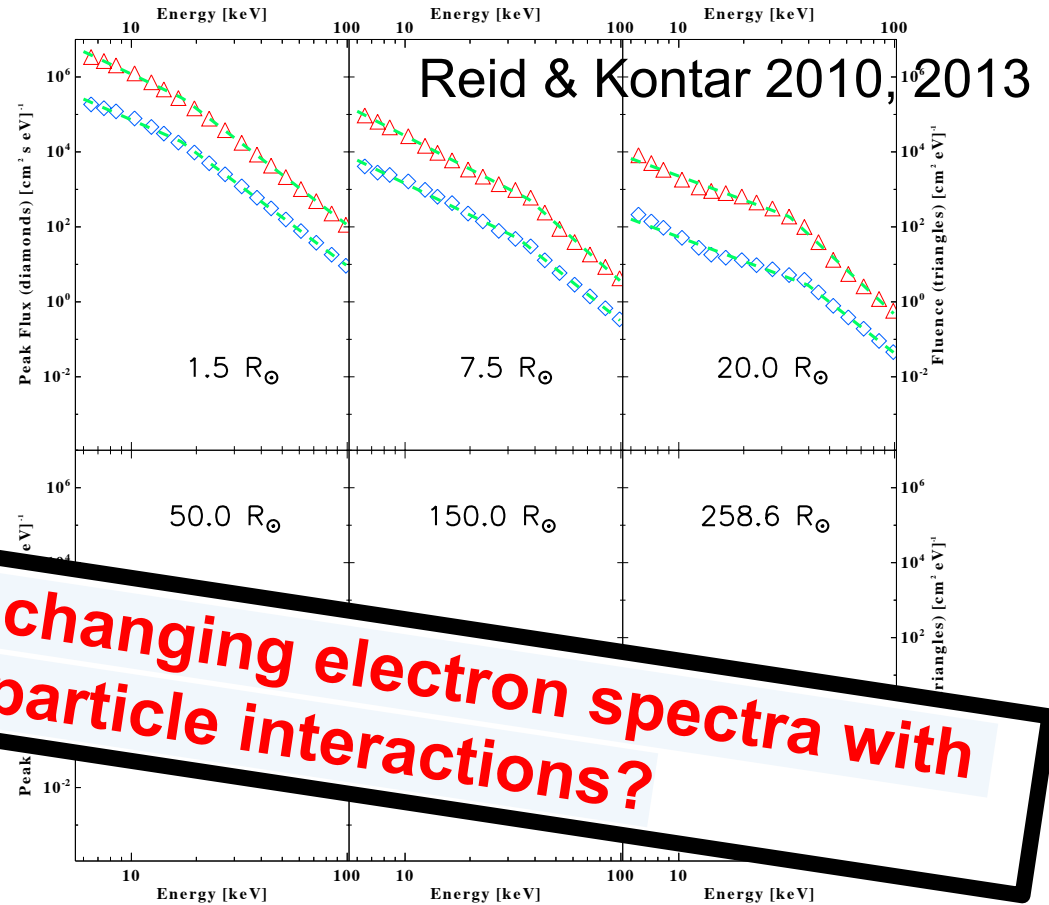
Peak
Flux

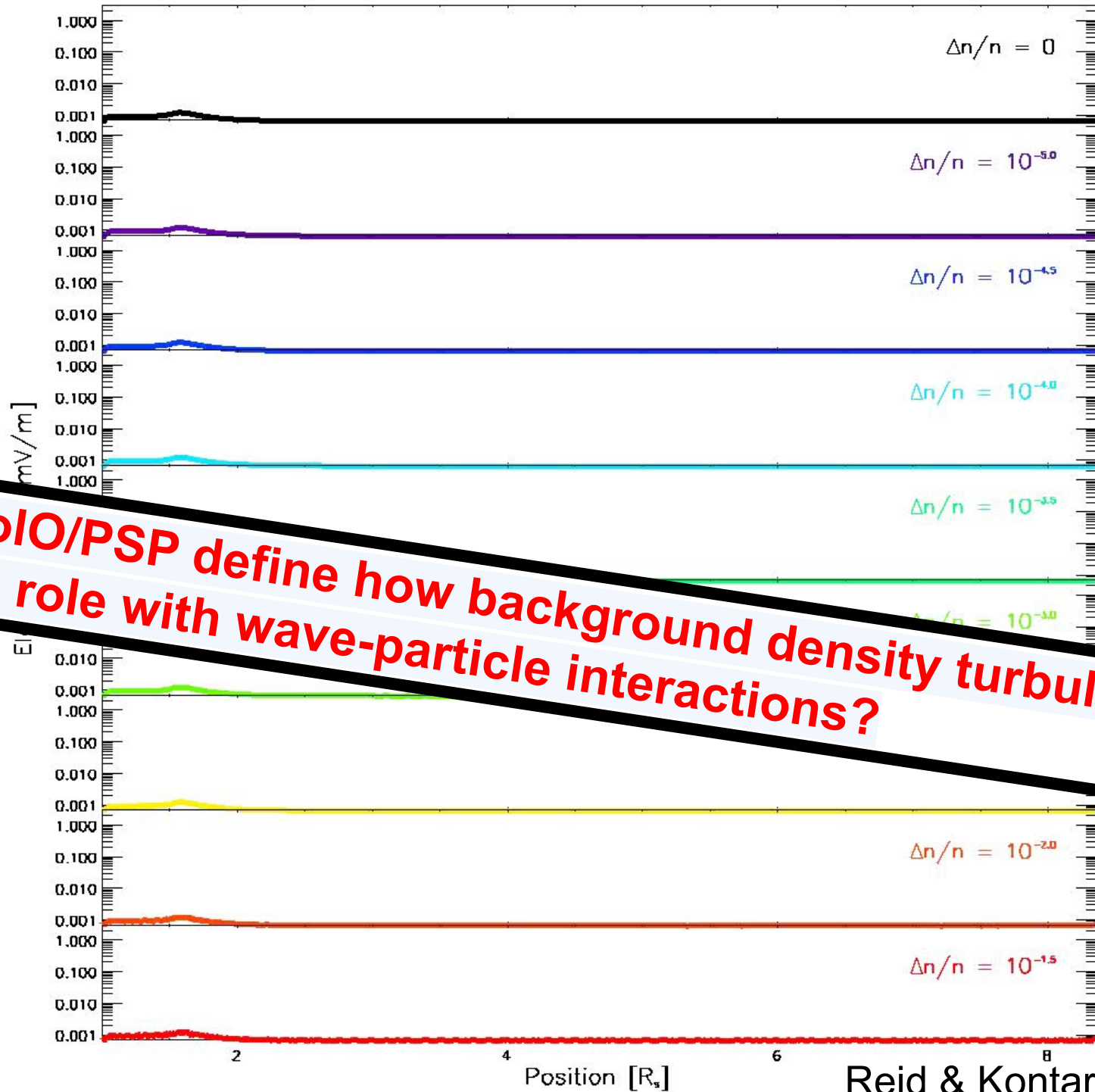


Fluence
(Flux, Time Integrated)



- Ratio of higher to lower spectral index depends upon the level of density turbulence in the plasma





Can SoLO/PSP define how background density turbulence plays a role with wave-particle interactions?